EFFECT OF SOLAR IRRADIANCE FLUCTUATIONS ON S-NPP REFLECTIVE BAND CALIBRATION

Yelena M. Savranskaya, Josef M. Wicker, Evan M. Haas, Jason C. Cardema, and Frank J. De Luccia*
The Aerospace Corporation, El Segundo, California

1. INTRODUCTION

The Visible-Infrared Imaging Radiometer Suite (VIIRS) is a multi-disciplinary sensor launched on-board of the Suomi National Polar-Orbiting Partnership (S-NPP) spacecraft on October 28, 2011. VIIRS mission is to collect measurements of clouds, aerosols, ocean color, surface temperature, fires, and albedo. It weighs approximately 275 kg with an average power consumption of 200Watts. The VIIRS design includes three major parts: a rotating telescope assembly (RTA), a solar diffuser (SD) assembly and on-board black body calibration source.

The instrument has 22 spectral bands: 14 reflective solar bands (RSB), 7 thermal emissive bands (TEB), and a Day Night Band (DNB). This paper will only concentrate on RSBs, practically their calibrations. The RSBs span wavelengths from 412 nm to 2250 nm, which are calibrated by using solar radiance reflected from a Solar Diffuser (SD). The SD reflectance degrades over time, and a Solar Diffuser Stability Monitor (SDSM) is used to track the changes. The ratio between the calculated solar radiance reflected from the SD and the VIIRS measurement of this radiance using the pre-launch calibration coefficients is known as the "F Factor".

Since VIIRs is expected to meet its mission requirements, the sensor calibration is important. Hence, there is a strong motivation to understand any "F Factor" fluctuations or variance.

2. BACKGROUND

"F Factor" is a measure of sensor degradation. It is calculated in post-processing for each RSB detector, de-trended, and stored in Lookup Tables (LUTs). It is the ratio between the calculated irradiance and the irradiance measured by the sensor during calibration. Equation 1 gives the definition of F Factor from Cardema, et al. (2012).

$$F = \frac{L_{calc}}{L_{meas}} \tag{1}$$

$$L_{calc} = \frac{P_{SUN}}{4\pi d_{SE}^2} \tau_{SDS} \cos\left(\theta_{SUN\_SD}\right) \Gamma_{BDRF} BRDF \tag{2}$$

The first term in Eq. 2 is the total irradiance of the sun at a distance of d_{SE}, with P_{SUN} the total radiant power of the sun. The transmission of the solar diffuser screen is τ_{SDS}, and θ_{SUN_SD} is the angle of incidence of the solar vector upon the diffuser screen. BRDF is the bi-directional reflectance distribution function of the solar diffuser, and Γ_{BDRF} represents the degradation of the BRDF. Computed solar irradiance is a function of the angle at which the solar vector is incident upon the solar diffuser. In 2014, an error was reported for the on-board software which calculates solar vectors used for F Factor computations. Specifically, an ECI-TOD (Earth Centered Inertial-True of Date) transformation was used to transform the solar vector into the instrument frame, instead of ECI-J2000. The current study computed solar vectors in post-processing using correct (J2000) coordinate transformation, along with ephemeris and attitude data from spacecraft telemetry (Spacecraft Diary files). Given the spacecraft ephemeris and attitude telemetry, the Satellite Orbit Analysis Program (SOAP) program was used to simulate the spacecraft motion and to compute solar vectors at the calibration collect times reported in the OBCIP (On-Board Computer Intermediate Product) files. The solar vectors thus computed were then used in place of those provided by VIIRS in the OBCIP files.

In 2013, the F Factors of several visible bands were found to exhibit unexpected fluctuations, and a spectral analysis indicated significant content at a frequency of one cycle per 1.5-2 weeks. VIIRS has an orbital period of only ~100 minutes. One hypothesis considered variability in solar irradiance as a possible source for the F Factor fluctuations.

* *Corresponding author address*: Frank J. De Luccia, The Aerospace Corporation, M1-013, El Segundo, CA 90245; e-mail: Frank.J.DeLuccia@aero.org

The F Factor computation currently assumes solar irradiance is constant. The results from the spectral analysis of F Factor fluctuations motivated a study of the correlation between F Factor and Total Solar Irradiance (TSI) measurements. Because F Factors are computed individually for each of the various spectral bands on VIIRS, correlation with Spectral Solar Irradiance (SSI) measurements is also considered.

Total Solar Irradiance (TSI) comprises contributions from the entire solar spectrum. TSI variations have long and short timescales. Long term variations are approximately 0.01% about a mean of 1366 W/m^2 over the 11-year solar magnetic cycle. The short term variations occur at time scales as short as a few days, with fluctuations up to 2-3 times larger than seen over the long term. Such amplitude of fluctuation is significant for the VIIRS RSB calibration stability goal of 0.1%, as referenced from Haas, et al. (2012). Variability in solar irradiance at periods of days to weeks is attributed to the combined effects of solar rotation (Carrington rotation period = 27.3 days) and the evolution of solar surface features (sunspots and bright faculae), which affect the radiant power measured from the sun, as pointed out in Ermolli, et al. (2013). Spectral Solar Irradiance (SSI) is the amount of the solar radiation in a specific range of the spectrum.

Several domestic and international missions were identified that collect TSI and/or SSI. The first mission is the Solar Radiation and Climate Experiment (SORCE). This NASA-sponsored satellite has four instruments on a LEO (Low Earth Orbit) satellite, including TSI and SSI sensors. The second mission is the ESA/NASA-sponsored Solar and Heliospheric Observatory (SOHO), whose platform flies a halo orbit about the first Lagrange point of the Earth-Sun system. Of SOHO's twelve different instruments, the Variability of Solar Irradiance and Gravity Oscillations (VIRGO) instrument provides TSI and SSI data. The third mission, Active Cavity Radiometer Irradiance Monitor Satellite (ACRIMSAT), is another NASA-sponsored satellite whose only instrument, ACRIM3, measures TSI from LEO.

Several steps were taken to investigate the impact which solar irradiance fluctuations may have on VIIRS calibration. First, missions that have collected TSI/SSI during NPP operations (starting from launch date of 28 Oct 2011 to present) were identified. Second, research instruments' accuracy and data reduction processes were evaluated. Third, TSI and SSI patterns were studied to identify variations within a data set from each instrument. Fourth, Fast Fourier Transfer (FFT) analysis on F Factor time series and TSI data was performed. Finally, the correlation between F Factor time series and TSI/SSI was investigated.

Several constraints impacted our analysis

1) the data availability during NPP operations (not enough missions, some missions ended)
2) data quality (longer missions had sensor degradation)
3) data reduction processes (variability in data reduction quality)

3. RESULTS

ACRIM, SORCE, and VIRGO were identified for TSI (Total Solar Irradiance) data, and overlaid in Figure 1a and 1b. Apart from slight differences in bias, the data shows consistency between the disparate sensors.

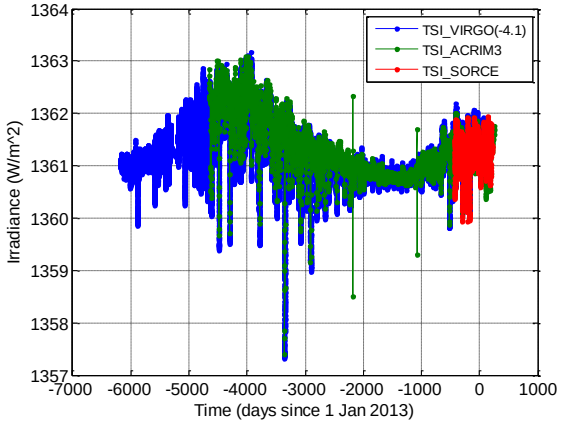

Figure 1a. TSI datasets.

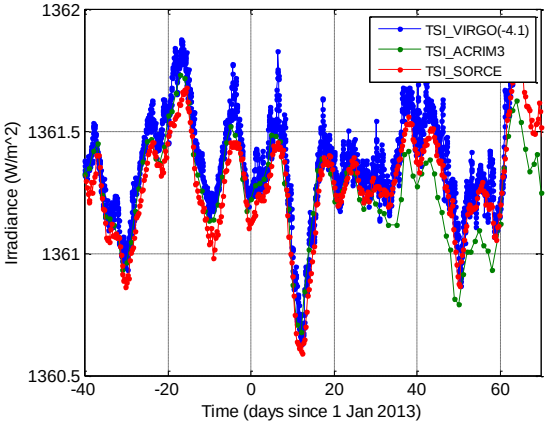

Figure 1b. Zoom of TSI dataset fluctuations showing consistency across disparate data sources.

Figure 2a and 2b compare the spectral content of the VIIRS F Factor for the M4 band (555nm center wavelength) with the spectral content of the ACRIM3 TSI data. The magnitude of the FFT (Fast Fourier Transform) of each dataset is plotted for the time interval spanning 1 Mar 2013 to 1 Apr 2013, with both datasets showing strong spectral content at a period of ~11 days.

Figure 3 plots the sample Pearson correlation coefficient between the variations in TSI ACRIM3 data and those in the F Factor for various VIIRS sensor bands. The sample correlation coefficient is computed as in Eq. 3 for two n-sample datasets, x and y:

$$r(x,y) = \frac{\sum_{i=1}^{n}(x_i - \mu_x)(y_i - \mu_y)}{\sqrt{\sum_{i=1}^{n}(x_i - \mu_x)^2 (y_i - \mu_y)^2}} \qquad (3)$$

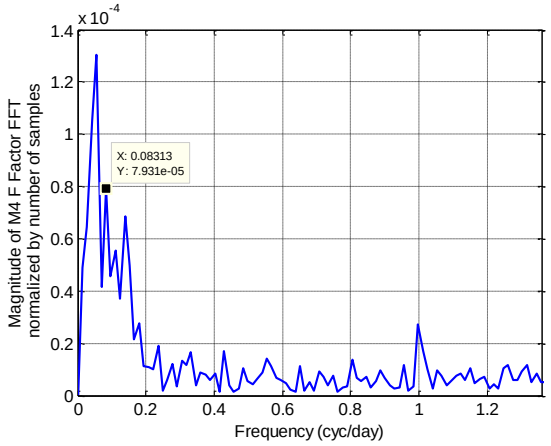

Figure 2a. M4 F Factor showing ~11-day cycles.

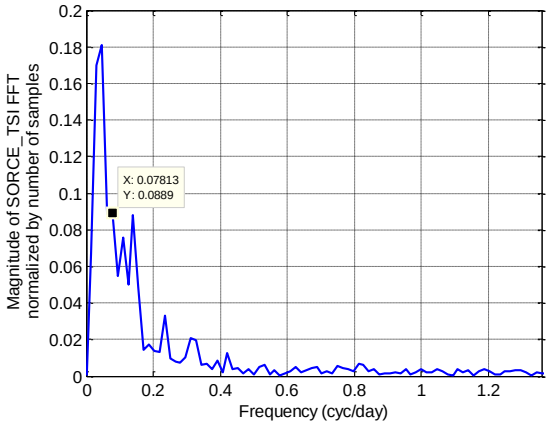

Figure 2b. ACRIM3 TSI data showing similar spectral content as M4 F Factor.

where μ_x and μ_y are the mean values of x and y, respectively. The data span June 2012-March 2013. Here one dataset is the variations in the detrended F Factor (denoted by ΔF), and the other dataset is the relative variation in the reciprocal of the solar irradiance data as given in Eq. (4).

$$\delta TSI(t) = \frac{mean(TSI(t))}{TSI(t)} - 1 \qquad (4)$$

The reciprocal of the solar data is used here, since an inverse relationship with F Factor is expressed in Eq. (1). The detrended ΔF values were obtained by fitting a low frequency least-squares spline to the post-calibration F Factors, F_{fit}, and then computing the normalized fluctuations about this fit:

$$\Delta F(t) = \frac{F(t)}{F_{fit}(t)} - 1 \qquad (5)$$

The spline fit was generated using knots evenly spaced at six weeks, so the F Factor variations are effectively high-pass filtered in F_{fit}.

The correlation is most pronounced in the higher frequency (lower wavelength) bands, which is to be expected based on Ermolli, et al. (2013). The F Factor data for all detectors in each band (using HAM A-side and gain 1) were averaged before computing the correlation. Also, the solar and VIIRS datasets were first interpolated onto a common timescale, and low-pass filtered with a 1cycle/day 4-pole Butterworth filter. Furthermore, a 16-day window near -66 days was excluded from the calculation of correlation coefficient, due to a large apparent artifact which especially impacted M7 F Factor data. This artifact may be due to a discrete update to the F Factor calibration, as per the process described in Haas, et al. (2012). Figure 4 examines the correlation of M4 with TSI_ACRIM3 in more detail, by computing the local correlation coefficient for a 6-week wide sliding data window. This "local" correlation can be quite strong, as shown for a ~3-month period in Figure 4, with local correlation coefficients above 0.8 for a significant amount of time. Figure 4 also shows the time-variations in the F Factor fluctuations overlaid with the relative solar irradiance variations. The variation of local correlation coefficient over the broader time range is plotted in Figure 5. Overall the correlation is quite strong, generally above 0.7. Computations of the six-week local correlation coefficient do not ignore the 16-day window surrounding the artifact near -66 days.

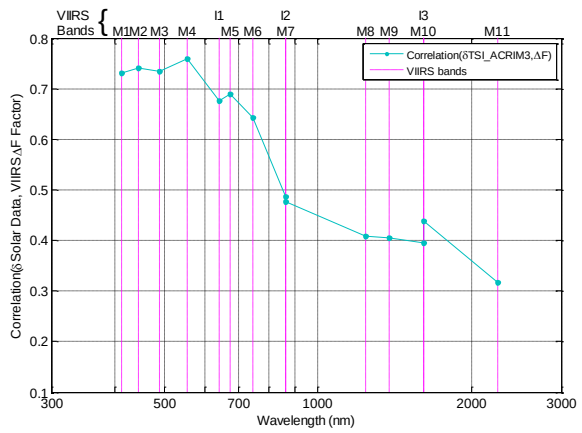

Figure 3. Correlation coefficient between TSI_ACRIM3 and VIIRS F Factor for various sensor bands.

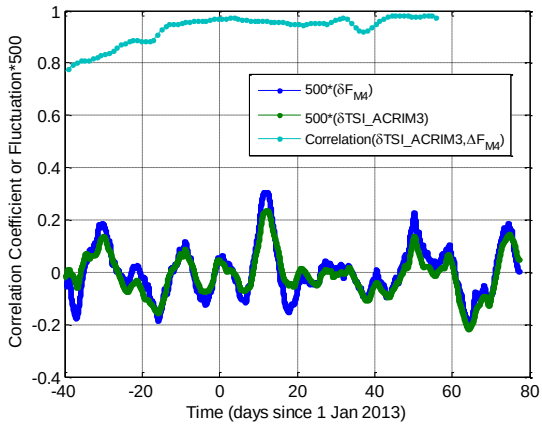

Figure 4. Local correlation of TSI_ACRIM3 data with VIIRS M4 F Factor indicating sustained region of strong correlation between the respective time series.

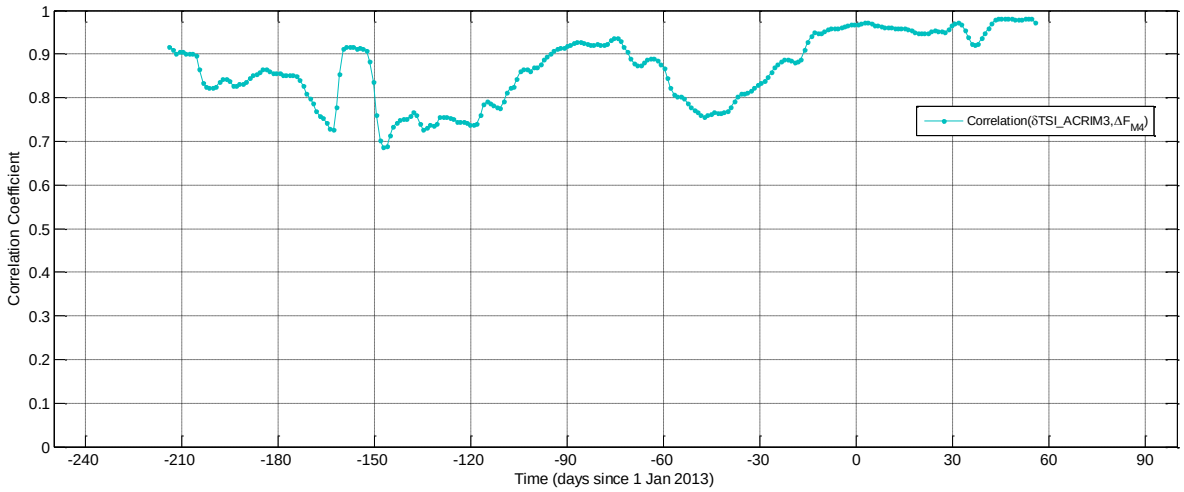

Figure 5. Local correlation coefficient between TSI ACRIM3 and M4 F Factor, showing good correlation overall, but with two regions of poor correlation (near -150 days and -50 days).

Figure 6 plots the Solar Spectral Irradiance (SSI) from two data sources: VIRGO SPM and SORCE SIM. Only the VIRGO SPM data will be used in comparison with VIIRS F Factor data, so this comparison serves to gain confidence in the VIRGO data. The VIRGO SPM sensor measures SSI at only three wavelengths: 402 (blue), 500 (green) and 862nm (red), while the SORCE data provide spectral resolution down to 0.4-4nm in the same region of the spectrum. The SORCE spectrum was therefore interpolated onto the three VIRGO bands. The comparison shows good agreement between the relative variations in both datasets. It should be noted that the VIRGO sensor's sensitivity has degraded substantially since the start of its operations in 1996, as described in Frohlich, et al. (2002), with the blue channel most significantly affected, currently showing less than 10% of its original gain. Also, the slight time shift which appears to exist may be due to fine time corrections which have not been applied here in processing the SORCE data.

The correlation between the SSI VIRGO data and the VIIRS F Factors are shown in Figure 7 for several sensor bands. Also plotted are the TSI correlation results from Figure 3. The SSI also shows higher correlation in the UV region, but not as strong as seen with the TSI data.

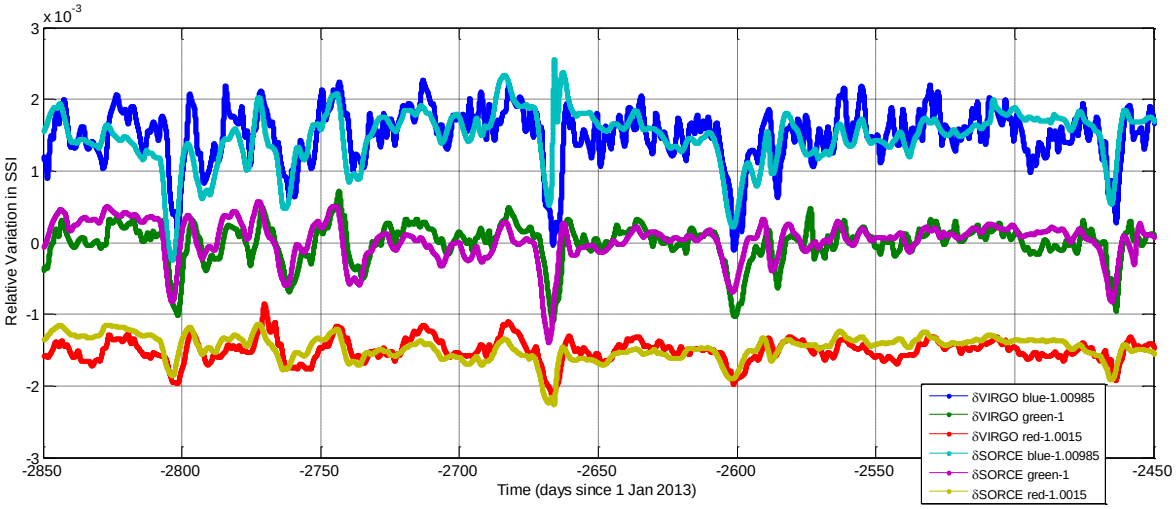

Figure 6. Comparison of relative variation in VIRGO and SORCE Solar Spectral Irradiance (SSI) data. Note small vertical shifts applied to datasets to blue and red datasets to allow plotting on a single graph.

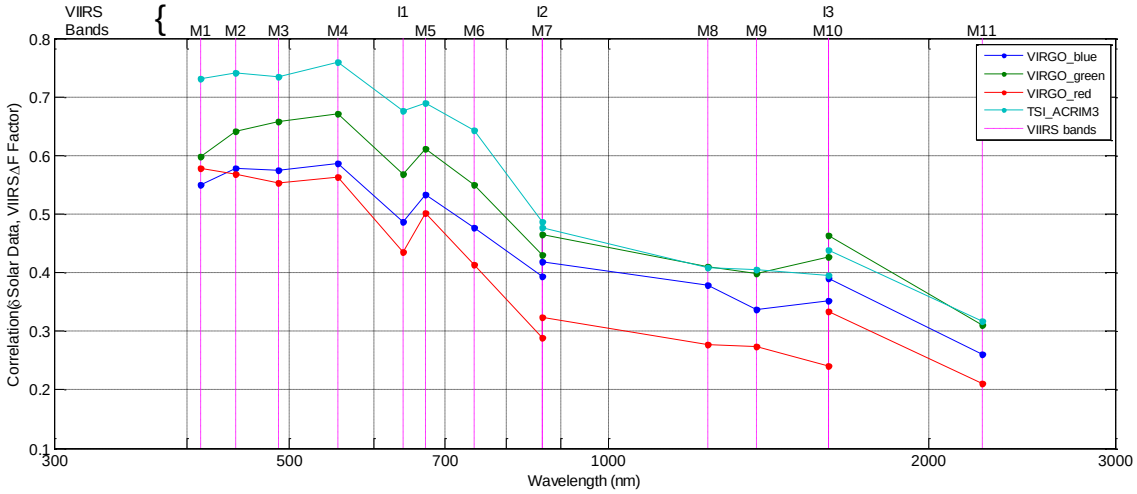

Figure 7. Correlation coefficient between SSI VIRGO data and VIIRS F Factor, along with previous TSI ACRIM3 results.

Figure 8 plots the local correlation coefficient for a six-week sliding window between the SSI VIRGO data and the M1, M3, and M7 F Factors of the VIIRS bands which are, respectively, nearest VIRGO's blue, green and red bands (the associated VIRGO/VIIRS bands have wavelengths of VIRGO blue/M1 = 402/412nm, VIRGO green/M3 = 500/488nm, and VIRGO red/M7 = 862/865nm). Also, the three VIRGO bands have narrower bandwidths (about 5nm) than the associated VIIRS bands (20-40nm). The previous local correlation between the TSI and M4 F Factor fluctuations is also plotted. None of the SSI correlations are clearly stronger than the TSI correlation, and the correlation of the VIRGO red band with M7 is significantly worse than the other correlations.

The correlations between the SSI components themselves and the TSI data are shown in Table 1. The correlation between the SSI bands, especially the blue and green, is quite strong. This indicates that all the wavelengths of interest see similar types of fluctuations. This is reflected in the consistent correlation with the TSI data over the three bands. The fairly high correlation between SSI and TSI data also indicates that the variations in the TSI data are quite similar to those of the SSI data. This appears to be supported by the multivariate

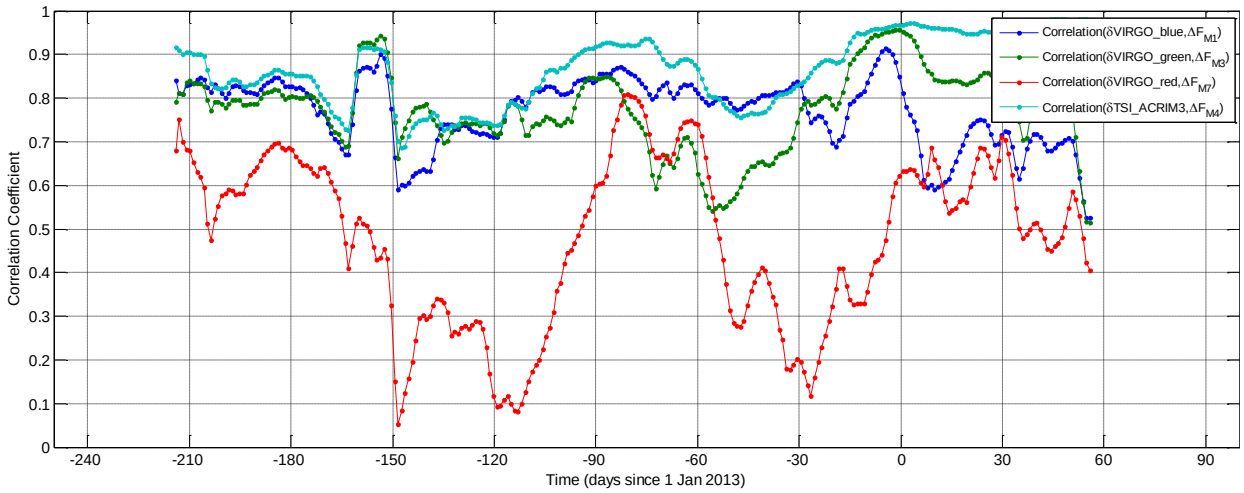

Figure 8. Local correlation coefficient between SSI VIRGO SPM data and respective VIIRS F Factors, along with previous correlation between TSI ACRIM3 TSI and M4 F Factor.

	SSI VIRGO Blue	SSI VIRGO Green	SSI VIRGO Red	TSI ACRIM3
SSI VIRGO Blue (402nm)	1	0.9037	0.8544	0.7067
SSI VIRGO Green (500nm)	0.9037	1	0.9204	0.7457
SSI VIRGO Red (862nm)	0.8544	0.9204	1	0.7199
TSI ACRIM3	0.7067	0.7472	0.7199	1

Table 1. Correlation matrix for SSI and TSI datasets, showing strong correlation among the blue, green and red components, and similar correlation between the SSI and TSI fluctuations.

spectral analysis of Ermolli et al. (2013), which concluded that 97% of the variance of TSI can be explained by a combination of the blue, green and red channels (for timescales smaller than about 130 days).

4. SUMMARY

The Visible-Infrared Imaging Radiometer Suite (VIIRS) launched on-board the Suomi National Polar-orbiting Partnership (S-NPP) spacecraft has 22 spectral bands. Fourteen of these are reflective solar bands (RSBs), which cover wavelengths from 412-2250nm. The RSB band calibration involves the "F Factor", which is the ratio between a reference solar radiance measurement and the VIIRS measurement using the pre-launch calibration coefficients. This paper has examined observed F Factor fluctuations and investigated their cause. Temporal variations in Total Solar Irradiance (TSI) have been shown to exhibit similar temporal frequency content as that seen in the F Factor variations. These timescales ~(days-weeks) are attributed to the combination of solar rotation and solar surface activity (i.e., sunspots and faculae). The fact that VIIRS F Factor calibration occurs on a weekly schedule motivates the consideration of these variations in solar irradiance, as does the amplitude of the variations, which can exceed the RSB F Factor calibration goals of 0.1% stability (depending mainly on the phase of the 11-year solar cycle). Further examination has revealed significant correlation between the temporal variations in TSI data (ACRIM3 sensor) and the F Factors for VIIRS bands, especially in the visible region ~(400-750nm). Spectral Solar Irradiance (SSI) data from the VIRGO SPM sensor are also considered. Good agreement between this SSI data and the SORCE SIM SSI sensor was observed over a data window for which both VIRGO and SORCE SSI data are available, but which pre-dates VIIRS. The VIRGO SSI data (at three wavelengths: blue=402nm, green=500nm, and red=865nm) were then correlated against the VIIRS F Factor data. Qualitatively similar results were obtained as for the TSI correlations. This suggests that other sources of F Factor variability may be more important than band-specific (i.e.,

wavelength-dependent) details of VIIRS's response to the Total Solar Irradiance fluctuations.

5. REFERENCES

Cardema, J. C., Rausch, K. W., Lei, N., Moyer, D. I., and De Luccia, F. J., 2012: Operational Calibration of VIIRS Reflective Solar Band Sensor Data Records. *Proc. SPIE*, Vol. 8510, 851019.

Ermolli, I., Mathess, K., Dudok de Wit, T., Krivova, N. A., Tourpali, K., Weber, M., Unruh, Y.C., Gray, L., Langematz, U., Pilewskie, P., Rozanov, E., Schmutz, W., Shapiero, A., Solanki, S. K., and Woods, T. N., 2013: Recent variability of the solar spectral irradiance and its impact on climate modeling. *Atmos. Chem. Phys.*, Vol. 13, 3945-3977.

Frohlich, C., and Wehrli, C., 2002: Variability of Spectral Solar Irradiance from VIRGO/SPM Observations. *Physikalish-Meteoroligisches Observatorium Davos,* World Radiation Center internal report.

Haas, E., Moyer, D., De Luccia, F., Rausch, K., and Fullbright, J., 2012: VIIRS Solar Diffuser Bidirectional Reflectance Distribution Function (BRDF) degradation factor operational trending and update. *Proc. SPIE*, Vol. 8510, 851016.